

# The ultra-deep XMM survey in the CDFS: X-ray spectroscopy of heavily obscured AGN

Andrea Comastri & the XMM-CDFS Team

INAF – Osservatorio Astronomico di Bologna, Via Ranzani 1, I-40127 Bologna, Italy  
e-mail: andrea.comastri@oabo.inaf.it

**Abstract.** We present selected results on the X-ray spectroscopy of distant, obscured AGN as obtained with the ultra-deep ( $\approx 3$  Ms) XMM-*Newton* survey in the Chandra Deep Field South (CDF-S). One of the primary goals of the project is to characterize the X-ray spectral properties of heavily obscured and Compton-thick AGN over the range of redshifts and luminosities that are relevant in terms of their contribution to the X-ray background. The ultra-deep exposure, coupled with the XMM detector's spectral throughput, allowed us to accumulate X-ray spectra for more than 100 AGN and to investigate the absorption distribution up to  $z \sim 4$ .

**Key words.** X-rays: galaxies – Galaxies: active – X-rays: diffuse background

## 1. Introduction

The advent of *Chandra* and XMM-*Newton* has revolutionized our knowledge of the hard X-ray sky. Active Galactic Nuclei are by far the dominant population and, thanks to many dozens of X-ray surveys covering a wide portion of the flux vs. solid angle plane, they can be studied over a large range of redshifts, luminosities and obscuring column densities. While the ultra-deep *Chandra* surveys (Xue et al., 2011) have reached flux limits where the Cosmic X-ray background is virtually completely resolved (see Gilli, these proceedings), most of the sources are detected with low counting statistic. The spectral throughput of the *pn* and MOS detectors on board XMM-*Newton* nicely complements deep *Chandra* observations and delivers X-ray spectra of unprecedented quality. The ul-

tra deep XMM-*Newton* survey was conceived to obtain good counting statistic for a sizable fraction of medium-bright AGN in the CDFS and its flanking fields over about  $0.3 \text{ deg}^2$ . One of the most important goals of the survey is the study of the relative fraction of heavily obscured and Compton thick AGN which is a key parameter of XRB synthesis models (Gilli et al., 2007; Treister et al., 2009).

## 2. The XMM ultra deep field: source detection and number counts

The effective exposure after background flares removal is about 2.82 and 2.45 Ms for MOS and *pn*, respectively. The final catalogues in the hard (2–10 keV) and very hard (5–10 keV) bands include 339 and 137 sources, respectively (Ranalli et al., 2013). The calculation of source counts and survey limiting fluxes ( $\approx 6.6 \times 10^{-16}$  and  $9.5 \times 10^{-16} \text{ erg cm}^{-2} \text{ s}^{-1}$  in

---

Send offprint requests to: A. Comastri

the hard and very hard bands, respectively), required extensive simulations to properly treat the various background components (cosmic, particle and soft protons) of XMM-Newton observations.

The large majority of XMM-Newton sources are also detected in deep Chandra images (Xue et al., 2011). Fifteen sources were not found in the Chandra catalogues and 8 of them lie in the deep 4 Ms area. A fraction of them are likely to represent the most extreme examples of obscuration. Multiwavelength follow-up observations are currently on going. The 2–10 keV flux distribution of the XMM-Newton sources is reported in Fig. 1 and compared with that obtained from the  $\sim 1$  Ms XMM-Newton survey in the Lockman Hole (Brunner et al., 2008) and the 4 Ms Chandra catalogue (Xue et al., 2011). While Chandra observations reach very low fluxes a larger number of objects at fluxes close to the knee of the luminosity function  $L_X \sim 10^{44}$  erg s $^{-1}$  at  $z \sim 1 - 2$  are obtained with XMM-Newton.

### 3. Deep X-ray spectroscopy

The search for and the characterization of the most obscured and Compton-thick AGN is pursued by exploiting the XMM-CDFS spectral catalogue, with different but complementary approaches including **i**) spectral fitting of individual sources, **ii**) colour-colour analysis and **iii**) stacking.

**i**). The X-ray spectral analysis of the candidate Compton-thick AGN from the first Ms of Chandra observations (Norman et al., 2002; Tozzi et al., 2006) revealed the unambiguous presence of Compton-thick features in two objects at  $z=1.53$  and  $3.70$  (Comastri et al., 2011). Further examples are reported in Georgantopoulos et al. (2013) where candidates are selected on the basis of X-ray properties, namely a flat ( $\Gamma < 1.4$  at the 90% confidence level) hard X-ray slope, suggestive of a reflection-dominated continuum, or the detection of a low energy turn over implying a column density  $> 10^{24}$  cm $^{-2}$ . There are nine candidates which satisfy the criteria above described. If the presence of significant iron K $\alpha$

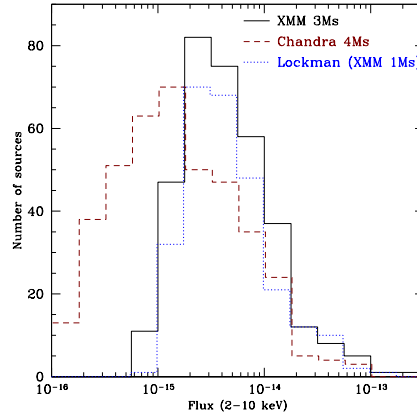


**Fig. 1.** The 2–10 keV fluxes of the XMM-CDFS sources (solid) compared with the Chandra (Xue et al. (2011), dashed line) and the XMM Lockman Hole (Brunner et al. (2008), dotted line) observations.

line is also required, the number of bona-fide Compton thick AGN is four. The four sources are equally distributed between transmission and reflection dominated. In Fig. 2 the spectrum of a transmission dominated source is reported. The best fit column density is  $\approx 1.1 \times 10^{24}$  cm $^{-2}$ , and the intensity of the iron line is of the order of 400 eV (rest-frame). An example of a reflection dominated AGN is shown in Fig. 3. A strong iron line, with a rest-frame Equivalent Width of  $\sim 1.2$  keV is clearly seen on top of a very flat continuum. Three of them are in the redshift range  $\approx 1.2-1.5$  and the remaining one at  $z=3.7$ .

**ii**). A complementary approach, devised to uncover heavily obscured AGN at relatively high redshifts, is described in Iwasawa et al. (2012). If the intrinsic continuum pierces through a high column density ( $N_H \geq 10^{23.5-24}$  cm $^{-2}$ ), an excess in the  $\sim 10-20$  keV energy range, with respect to lower energies, is clearly evident. The rest-frame high energy ( $> 10$  keV) emission enters the XMM-Newton hard X-ray band for the 46 sources at  $z > 1.7$ . Using an X-ray colour-colour diagram based on carefully chosen rest-frame bands (Fig. 4), the sources are classified on the basis of their spectral hardness on Very obscured

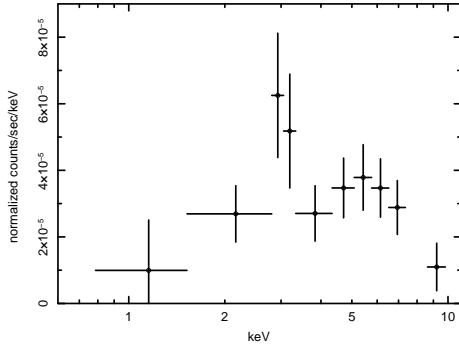


**Fig. 2.** The *pn* X-ray spectrum of the Compton thick source PID-66 at  $z=1.185$

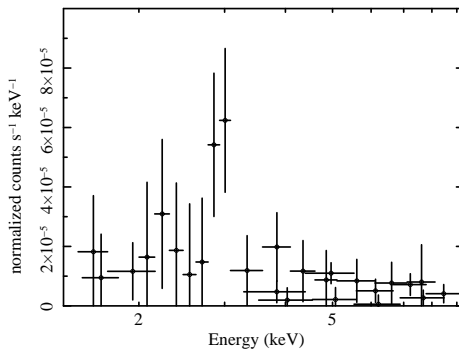


**Fig. 3.** The *pn* and MOS X-ray spectrum of the reflection dominated AGN PID-324 at  $z=1.222$

(V), Absorbed (A), Mildly obscured (M) and Unobscured (U). Seven sources fall in the V category. The column densities as measured by spectral fitting are in the range  $0.4-1 \times 10^{24} \text{ cm}^{-2}$ .

Their average redshift ( $z \approx 2.7$ ) and 10–20 keV luminosity ( $\log L_X \approx 44$ ) classify them as heavily obscured quasars. For none of them the column density is significantly larger than  $\sim 10^{24} \text{ cm}^{-2}$  although for two objects a reflection dominated spectrum provides an equally good description of the data.

iii). The stacking technique has been further employed to search for iron line spectral features in the X-ray spectra of 50 relatively bright sources covering about two decades in X-ray luminosities. The *pn* and MOS spectra are summed in the rest-frame 2–12 keV band; see Falocco et al. (2013) for a detailed dis-

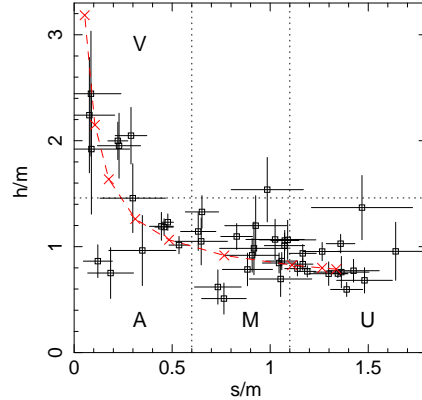


**Fig. 4.** The X-ray colour-colour diagram, where  $s$ ,  $m$  and  $h$  are the counts in the rest-frame bands of 3–5 keV, 5–9 keV and 9–20 keV, respectively. The red dashed-line indicates the evolution track of the X-ray colour when a power-law of  $\Gamma = 1.8$  is modified by various absorbing column. The crosses mark  $\log N_{\text{H}}$  values 21, 22, 22.5, 23, 23.3, 23.5, 23.7, 23.85 and  $24 \text{ cm}^{-2}$  from the bottom-right to the upper-left along the track.

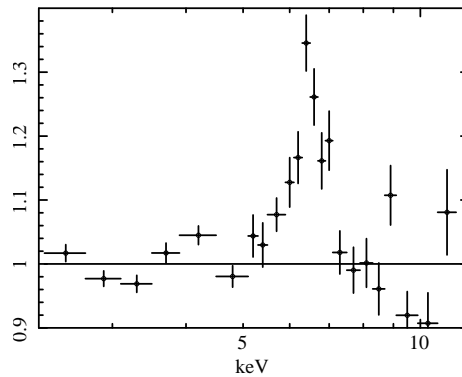


**Fig. 5.** The ratio with respect to a power law fit of the stacked spectrum of bright sources ( $S/N > 15$ ) with 2–10 keV luminosities lower than  $10^{44} \text{ erg cm}^{-2} \text{ s}^{-1}$

ussion. The residuals with respect to a single power law fit of the stacked spectrum of two sub-samples, splitted according to the X-ray luminosity, with a threshold at  $10^{44} \text{ erg s}^{-1}$ , are reported in Fig. 5 and 6. A highly significant feature at  $\approx 6-7 \text{ keV}$  is evident. The iron line intensity appears to be stronger in the low luminosity sample (Fig. 5). Moreover, the

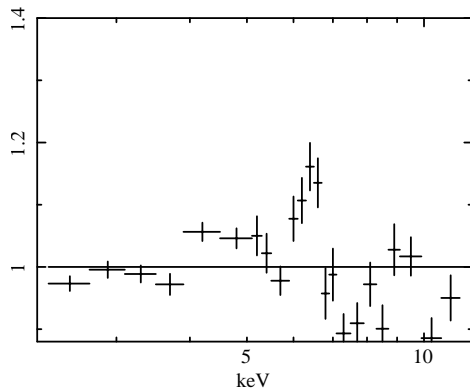


**Fig. 6.** As in Fig. 5, but for luminous QSOs. Spectral complexity, unaccounted for by a single power law, is clearly evident at energies  $> 7$  keV. Also note that the  $y$ -axis scale is the same as in Fig. 5.

shape of the residuals suggests the presence of a broad red wing extending to about 5 keV, and of a narrow component at 6.4 keV, with an Equivalent Width of  $\approx 100$  and 50 eV respectively. However the improvement in the fit quality adding a relativistic component is of the order of  $2\sigma$ . In order to constrain the presence and the intensity of possible relativistic features, a larger sample, including *Chandra* spectra, would be needed.

#### 4. Prospects for the near and mid-term future

The systematic analysis of the *XMM-Newton* spectra in the CDFS is in progress (Comastri et al., 2013). Despite the relatively high level of the instrumental background in the *XMM-Newton* CDFS deep field, the quality of the spectra is such to perform a detailed spectral analysis for a sizable sample ( $\approx 150$  objects) of relatively faint sources at moderate to high redshifts. Preliminary results, such as those briefly described above, seem to indicate a paucity of Compton-thick AGN with respect to heavily obscured ( $N_{\text{H}} \sim 10^{23-24} \text{ cm}^{-2}$ ) objects. Also, the detection of reflection dominated AGN with the same frequency of transmission dominated ones (albeit the statistic is poor) was somehow unexpected. Although

the present findings suggest that the sources of the 20–30 keV XRB peak may be different from what postulated by AGN synthesis models, a larger sample of heavily absorbed and Compton-thick AGN is needed. A systematic search for the most obscured AGN will be performed combining the *XMM-Newton* and the *Chandra* spectra and will require a careful modelling of the background to search for spectral features (iron features, low energy cut offs, ...) among faint X-ray sources.

A major step forward towards a proper characterization of hidden black holes will be given by NuSTAR (Harrison et al., 2013), on orbit since June 13, 2012, carrying the first focusing optics at  $E > 10$  keV. The deep NuSTAR survey in the CDFS will likely reach sensitivities of a few  $\times 10^{-14} \text{ erg cm}^{-2} \text{ s}^{-1}$  in the 10–40 keV range. While, it is unlikely that the NuSTAR deep surveys will discover new X-ray sources, they will help to put significantly better constraints on the  $N_{\text{H}}$  distribution, especially at  $z < 1 - 2$ . As far as the search for high- $z$  obscured AGN is concerned, additional deep *XMM-Newton* and ultra-deep *Chandra* surveys will remain a unique resource in the years to come.

*Acknowledgements.* I wish to thank the members of the CDFS collaborations for their help, and in particular P. Ranalli, C. Vignali & R. Gilli. Support from ASI-INAF grant I/009/10/0 and PRIN-INAF 2011 is acknowledged.

#### References

- Brunner, H., et al. 2008, *A&A*, 479, 283
- Comastri, A., et al. 2011, *A&A*, 526, L9
- Comastri, A., et al. 2013, *A&A*, in preparation
- Falocco, S., et al. 2013, *A&A*, submitted
- Georgantopoulos, I., et al. 2013, *A&A*, in press
- Gilli, R., et al. 2007, *A&A*, 463, 79
- Harrison, F. A., et al. 2013, *ApJ*, in press (arXiv:1301.7307)
- Iwasawa, K., et al. 2012, *A&A*, 546, A84
- Norman, C., et al. 2002, *ApJ*, 571, 218
- Ranalli, P., et al. 2013, *A&A*, in press
- Tozzi, P., et al. 2006, *A&A*, 451, 457
- Treister, E., et al. 2009, *ApJ*, 696, 110
- Xue, Y. Q., et al. 2011, *ApJS*, 195, 10